forests

MDPI

Article

Seasonal, Monthly, Daily, and Diel Growth, and Water Status Dynamics of Balsam Fir in a Cold and Humid Boreal Environment

Shalini Oogathoo [1,2,*], Louis Duchesne [3], Daniel Houle [4], Daniel Kneeshaw [1] and Nicolas Bélanger [1,2]

[1] Centre d'Étude de la Forêt, Université du Québec à Montréal, Case Postale 8888, Succursale Centre-Ville, Montréal, QC H3C 3P8, Canada
[2] Data Science Laboratory, Université du Québec (TÉLUQ), 5800 rue Saint-Denis, Bureau 1105, Montréal, QC H2S 3L5, Canada
[3] Direction de la Recherche Forestière, Ministère des Ressources Naturelles et des Forêts du Québec, 2700 Einstein, Quebec City, QC G1P 3W8, Canada
[4] Science and Technology Branch, Environnement et Changement Climatique Canada, 105 McGill St., Montreal, QC H2Y 2E7, Canada
* Correspondence: shalini.oogathoo@gmail.com

Abstract: Despite new knowledge in recent years, our understanding of the phenology of wood formation for various species growing in different environments remains limited. To enhance our knowledge of the tree growth dynamics of boreal tree species, we investigated the average seasonal, monthly, daily, and diel patterns of tree growth and water status from 11 years of observations with the 15 min and 1.5 µm resolved stem radial size variation data of 12 balsam fir (*Abies balsamea* (L.) Mill.) trees growing in a cold and humid boreal environment. Growth only occurred above an air temperature threshold of 9–10 °C, and the maximal growth rate over the year (23–24 June) was synchronous with the maximal day length (20–21 June) and not with the maximal air temperature, which occurred on average about 2 weeks later (4–5 July). Tree growth was mostly restricted by air temperature and solar radiation under these cold and wet boreal conditions, but our results also highlight a turgor-driven growth mechanism. Diel dynamics reveal that tree growth is minimal during the day when the stem dehydrates, and higher past midnight when the stem is fully rehydrated. This pattern suggests that carbon assimilation through photosynthesis occurs primarily during the day, while energy production and carbon allocation to woody tissues occur primarily at night via cellular respiration. Overall, our results show that the temporal patterns of the growth and water status of balsam fir growing in cold and humid boreal environments are controlled by a set of environmental factors that influence various physiological processes and mechanisms, many of which still need to be documented.

Keywords: point dendrometer; growth; rehydration; dehydration; stem radial variation; boreal tree species; balsam fir; diel and seasonal patterns

Citation: Oogathoo, S.; Duchesne, L.; Houle, D.; Kneeshaw, D.; Bélanger, N. Seasonal, Monthly, Daily, and Diel Growth, and Water Status Dynamics of Balsam Fir in a Cold and Humid Boreal Environment. *Forests* **2023**, *14*, 802. https://doi.org/10.3390/f14040802

Academic Editor: Roberto Tognetti

Received: 6 March 2023
Revised: 4 April 2023
Accepted: 11 April 2023
Published: 13 April 2023

1. Introduction

Terrestrial carbon (C) budgets show that forests have captured approximately one-third of anthropogenic carbon dioxide (CO_2) emissions in recent decades, which has contributed significantly to climate-change mitigation [1,2]. Given the major role of forest ecosystems in the C cycle, and their feedback loops with climate and atmospheric CO_2 concentration, it is essential to consider the evolution of terrestrial C pools and fluxes in global climate-change projections [3,4]. For this reason, an increasing number of dynamic global vegetation models (DGVMs) have been developed in recent years to simulate climate–vegetation dynamics, and to more realistically predict the evolution of water and energy fluxes, C cycling, and the climate [5–8]. On the basis of the predictions of these models, forests are expected to continue to behave as C sinks [9,10].

Despite significant advances in the field, some researchers have indicated shortcomings of DGVMs in correctly simulating tree and forest growth. One of the identified shortcomings is that current models simulate long-term tree and forest stand growth on the basis of photosynthesis and C assimilation, whereas C allocation in woody tissues and tree growth are potentially strongly constrained by environmental factors that differ from those that govern photosynthesis and C assimilation [11–16]. The fact that growth is driven by photosynthesis in existing DGVMs without considering water, thermal constraints, sunlight, and nutrient limitations to woody tissue production potentially results in an overestimation of future forest growth in response to increasing atmospheric CO_2 and temperature [13,15]. Thermal conditions, and light, water, and nutrient availability change over the growing season, and these temporal variations in resource availability all have the capacity to influence growth. Consequently, a revised hierarchy of plant growth control in DGVMs was proposed [11,12,17,18].

Proposed DGVM improvements rely mostly on the better understanding of environmental factors that govern tree growth and their representation in the models. Xylogenetic models that explicitly consider wood formation were suggested as a promising framework for incorporating climatic controls on tree growth into DGVMs [13]. However, knowledge on the influence of environmental factors on xylem formation and tree growth remains limited [13,19], and the translation of xylem formation processes in the tree to the forest at the stand, local, or regional scale in DGVMs remains a major challenge [16,20,21]. This is especially critical in cold and humid boreal environment where growing seasons are short and climate warming is expected to be large.

The study of cambial activity and xylem formation from the analysis of (1) repeatedly sampled microcores of newly formed xylem throughout the growing season or pinning techniques [13,22–27], and (2) data from repeatedly sampled dendrometric bands during the growing season [28,29] significantly contributed to our understanding of the environmental factors that regulate xylem formation and tree growth. At a higher temporal resolution, electronic dendrometer data were also used to characterise tree growth and water status [30–32]. Radial growth monitoring with dendrometers is a much less laborious method than the anatomical analysis of woody tissues is, and allows for continuous nondestructive monitoring at the same location on the tree stem. Although they are not associated with quantitative wood anatomy data, electronic-dendrometer data are useful in studying environmental controls on tree water status and growth dynamics. For example, the analysis of the diel growth dynamics of seven temperate tree species from 8 years of hourly resolved stem radial growth data provided insight into its mechanisms and key environmental drivers [31]. One of the main highlighted mechanisms is turgor-driven growth, according to which growth primarily occurs when wood tissues are water-saturated, and trees are not water-stressed [30,31,33,34]. These analyses were possible due to recent methodological developments and in particular the "zero growth" concept, according to which no growth occurs during periods of stem shrinkage. Using this concept, the high-resolution time-series datasets of stem radius variations can be partitioned into (1) a growth phase that begins when the previous maximal stem radius is exceeded, and ends when stem shrinkage occurs, and (2) a tree water-deficit phase that begins when the stem size decreases below a preceding maximum [30].

Despite all the new recent knowledge, our understanding of the phenology of wood formation for various species growing in different environments remains limited. Recently, the dynamics of seasonal radial growth of balsam fir trees growing in a cold and humid boreal environment was documented using dendrometric data over 12 years [35]. The results contribute to our knowledge of the seasonality of tree growth in boreal forests by showing that balsam fir (*Abies balsamea* (L.) Mill.) growth occurs over a short period of about 3 months, but 80% of it is achieved in the first 50 days of the growing season. The analysis revealed that the timing of growth cessation is the most important determinant of growing season length, while the timing of growth onset has less influence. These analyses also showed that the average growth rate of trees was higher during growing seasons that

ended early, and lower when the end of the growing seasons was stretched, meaning that longer seasons are not necessarily the most productive. To further enhance our knowledge of the tree growth dynamics of boreal tree species, our primary objective in this study was to investigate seasonal, monthly, daily, and diel growth, and tree water status dynamics from up to 11 years of observation with 15 min and 1.5 µm resolved stem radial variation data of 12 balsam fir trees growing in a cold and humid boreal environment. On the basis of current knowledge, we expected that, over the course of the year, growth would occur over a short period in the summer, mostly during June and July, a period characterized by air temperature above a to-be-determined threshold, and that diel, daily, and seasonal growth dynamics would follow day length, solar radiation, and vapour pressure deficit (VPD) patterns. We also expected the greatest variations in stem water status to occur outside of this period, primarily in the autumn, when stems dehydrate in preparation for the continuous period of below-freezing temperature, and in the spring, when temperatures warm and stems rehydrate prior to the onset of irreversible turgor-driven growth. For the diel dynamics, we expected that, during the growing season, trees would grow mostly at night, dehydrate during the day and rehydrate in the evening following solar radiation and the patterns of VPD. As a secondary objective, we aimed to test the use and contribute to the methodological development of the "zero-growth" concept for extracting tree growth and water status signals from the high-resolution time series datasets of stem radius variations.

2. Method

2.1. Instrumented Trees

We instrumented 12 balsam fir trees located in a mature forest of the Laurentian Wildlife Reserve, ~50 km north of Quebec City (47°19′31″ N; 71°07′43″ W, 740–760 m.a.s.l.), at the boundary of the Lac Laflamme watershed, which is one of the three study watersheds that are part of the Québec Forest Ecosystem Research and Monitoring Network (Réseau d'Étude et de Surveillance des Écosystèmes Forestiers; RESEF). The instrumented trees had a diameter at breast height (DBH) ranging from 14.0 to 22.8 cm in 2009, and are located in a 3600 m^2 experimental area that is characterized by sandy till soils overlaying Precambrian charnockitic gneiss bedrock and a terrain slope of 15%. The forest is dominated by balsam fir, with a small component of paper birch (*Betula papyrifera* Marsh.) and white spruce (*Picea glauca* (Moench) Voss), which is typical of forests found on mesic sites of the eastern balsam fir–paper birch bioclimatic subdomain in Quebec, Canada [36]. In order of importance, these species represent 93, 4, and 3% of the total stand basal area, respectively (i.e., 43 m^2 ha^{-1}) for trees with a diameter at breast height greater than 1 cm. With climate norms (1981–2010) of −0.18 °C and 1460 mm for mean annual air temperature and mean annual precipitation, respectively, the climate is classified as warm-summer humid continental according to the Köppen climate classification [37]. The experimental area underwent defoliation by the hemlock looper (*Lambdina fiscellaria*, Guenée) during the 2012–2014 period [38], whereas the 2012 defoliation was concurrent with a severe drought in the area in July of the same year [39].

The 12 trees were equipped with a radius dendrometer (model DR1, Ecomatik, Munich, Germany), orientated to the south and positioned at approximately 2 m from the ground to ensure being above the snow cover in order to track stem radial variations at a high temporal resolution (15 min) in a soil warming experiment initiated in 2009. The effects of this treatment on soil ion fluxes and mineralizable C, and on the xylogenesis and intra-annual growth of mature balsam fir trees were documented [35,40–43]. The soil warming treatment and dendrometric measurements have continued since the inception of the experiment in 2009. Thus, the high temporal resolution of tree radial variations that were monitored between August 2009 and October 2020 were used to document the average intra-annual and daily patterns of tree growth, and variations in water status. Given the relatively small documented effects of the soil warming treatment, we did not consider it in our compilations.

Five trees died in 2013 due to severe defoliation caused by the 2012–2014 hemlock looper outbreak, and the annual growth monitoring of three individuals was interrupted because of dendrometric malfunction due to ice formation in the sensors or because the potentiometer had reached its maximal stroke during the growing season [35]. Intra-annual and diel growth, and tree water status dynamics were lastly compiled from 3.1 million stem radius measurements over a period of more than a decade, encompassing up to 12 individuals depending on the considered period. The experimental design and yearly individual time series of radial measurements are detailed in [35].

2.2. Characterisation of Tree Growth and Water Status Changes from Dendrometric Data

The high-temporal-resolution signal of radial variations in the tree stems combines two distinct physiological processes: irreversible woody tissue growth and variations due to changes in tree water status. Since the definition of the "zero-growth" concept in which no growth occurs during periods of stem shrinkage [30], it is increasingly used for the analysis of high-temporal-resolution electronic-dendrometer data [31,32,35,44]. Using this concept, the signal of stem radial variation may be partitioned into (1) a growth (GRO) phase that begins when the previous maximal stem radius is exceeded and ends when stem shrinkage occurs, and (2) a tree water deficit (TWD) phase that begins when the stem radius decreases below a preceding maximum. We refined this approach by dividing the TWD phase into two distinct phases corresponding to stem shrinkage associated with woody tissue dehydration, and stem expansion associated with woody tissue rehydration. Thus, the high-temporal-resolution signal from the dendrometers was decomposed into three distinct signals (growth (G), dehydration (D), rehydration (R)):

$$G_t = \left\{ \begin{array}{ll} 0, & SR_t < max(SR_{<t}) \\ SR_t - SR_{t-1}, & SR_t \geq max(SR_{<t}) \end{array} \right\} \quad (1)$$

$$D_t = \left\{ \begin{array}{ll} 0, & SR_t \geq max(SR_{<t}) \bigvee SR_t \geq SR_{t-1} \\ SR_t - SR_{t-1}, & SR_t < max(SR_{<t}) \bigwedge SR_t < SR_{t-1} \end{array} \right\} \quad (2)$$

$$R_t = \left\{ \begin{array}{ll} 0, & SR_t \geq max(SR_{<t}) \bigvee SR_t \leq SR_{t-1} \\ SR_t - SR_{t-1}, & SR_t < max(SR_{<t}) \bigwedge SR_t > SR_{t-1} \end{array} \right\} \quad (3)$$

where SR indicates the stem radius recorded with the dendrometer, t refers to the current record, and $<t$ refers to historical records. Prior to signal decomposition, the raw 15 min dendrometric data were visually examined, and validated for any errors that could be manually removed and corrected, such as regarding jumps associated with dendrometric adjustment or replacement.

Individual cumulative hourly variations in stem radius associated with stem radial growth, dehydration, and rehydration were then calculated, and the average seasonal (winter: DJF; spring: MAM; summer: JJA; autumn: SON), monthly, daily, and diel dynamics over the entire period are reported.

3. Results

3.1. Dendrometric Signal Decomposition

Figure 1 shows the results of the signal decomposition of a high-resolution time series of radius dendrometer data (cumulative stem radius variations) into three distinct time series corresponding to daily stem radius variations associated with growth, dehydration, and rehydration for a given balsam fir tree and growing season. This approach also allowed for us to estimate the beginning of the growing season, defined as the time when the stem radius exceeds the maximal value recorded during the past year, and the end of the seasonal growth, considered the time when the maximal value is reached (Figure 1). These dates correspond to the beginning and end of irreversible growth, as measured with the dendrometers. However, this does not mean that the onset and cessation of growth determined from dendrometers corresponded exactly to the onset and cessation of

xylogenesis associated with cell division and maturation. It remains difficult to identify a detailed chronology at a high temporal resolution.

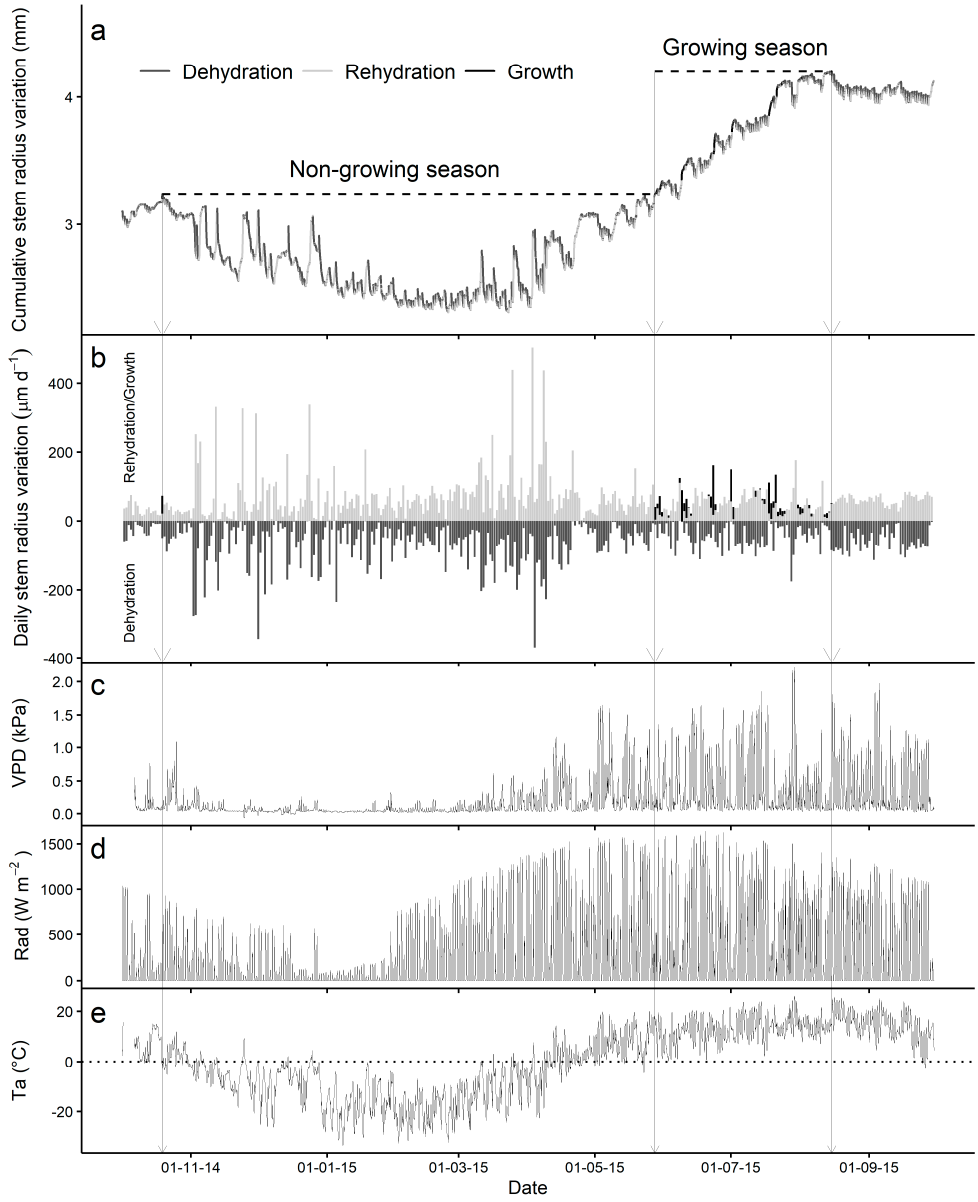

Figure 1. (**a**) Annual pattern of cumulative stem radius variation with 15 min intervals (mm) and (**b**) daily stem radius variation (µm day^{-1}) associated with growth and tree water status variations (dehydration and rehydration) for Tree 104 in 2014–2015, and (**c**) mean daily vapour pressure deficit (VPD), (**d**) solar radiation (Rad), and (**e**) air temperature (Ta) over the same period.

3.2. Average Daily and Monthly Patterns

Average daily and monthly patterns of stem radius changes associated with growth, dehydration, and rehydration are presented in Figure 2 (left column). For all years combined, the window of uninterrupted average daily growth started at DOY 142 (20–21 May), peaked at DOY 175 (23–24 June), and ended 118 days later, on DOY 260 (16–17 September). Almost half (44%) of the total annual growth of 1.3 mm was, however, achieved in 33 days between the beginning and the peak of the growing season at a mean growth rate of 16.7 µm day^{-1} or 0.7 µm h^{-1}. Considering the growth pulses of the low amplitude occasionally observed before and after the growing period, some in spring, but mostly in autumn, results reveal that growth occurred over a window of 183 days, i.e., half a year, while null growth is observed for an equivalent number of days per year. The monthly averages revealed that trees grew

6.1 and 3.6 times faster on average in June and July, respectively, compared to May and August.

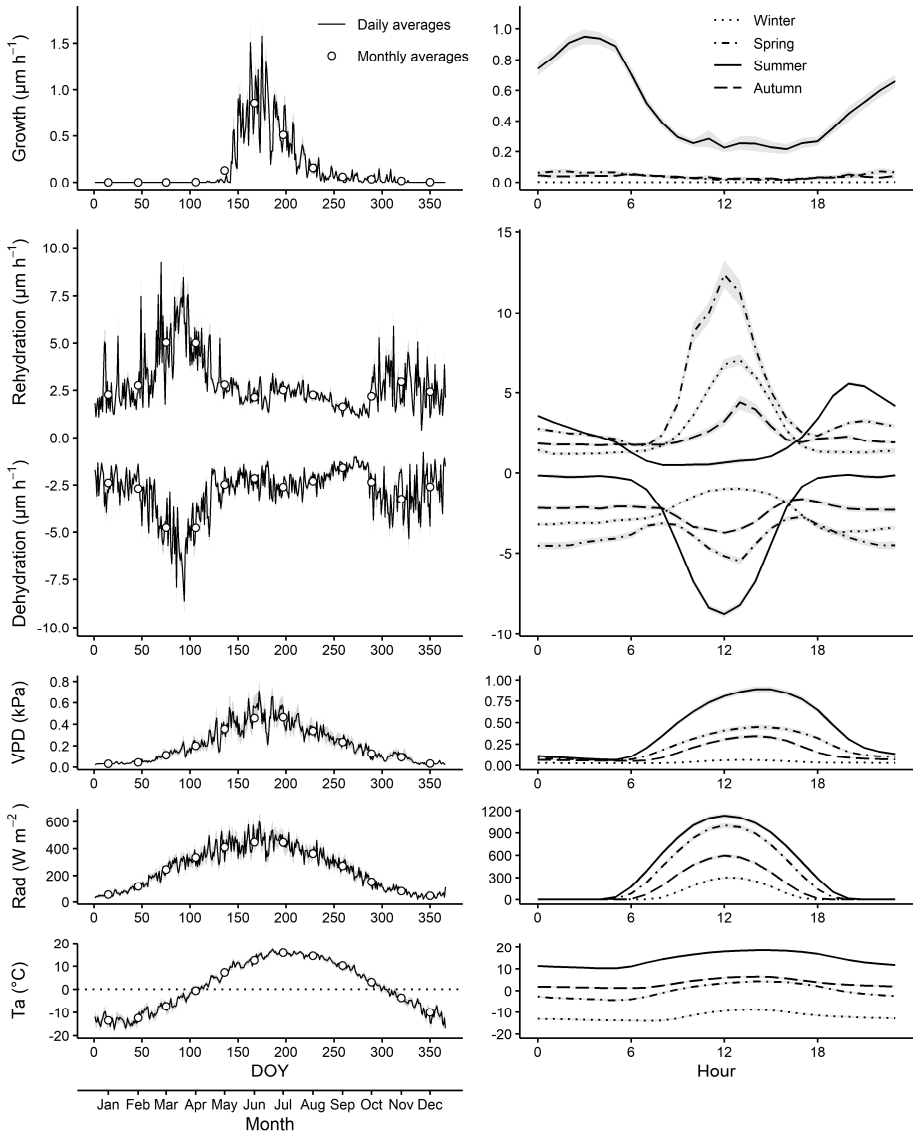

Figure 2. (**left**) Annual pattern of daily and monthly stem radius variation and (**right**) seasonal diel pattern associated with growth and tree water status variations (dehydration and rehydration) for all monitored trees (averaged) over the 11-year period (2009–2020) along with pattern of vapour pressure deficit (VPD), solar radiation (Rad), and air temperature (Ta) over the same period. Shaded area shows 95% confidence interval for the mean.

Over the course of the year, daily variations in tree water status were most pronounced during freeze/thaw transition periods in spring and autumn (particularly in spring), and had less amplitude during the growing season (Figure 2). Nevertheless, over the growing season (118 days, DOY 142 to 260), stem radius variations associated with changes in stem water status (dehydration and rehydration) were five times greater (±6.5 mm of cumulative shrinkage and swelling, ±54 µm days^{-1} on average) compared to the irreversible radial changes associated with growth (1.2 mm, 10 µm days^{-1} on average) over the same period (Figure 2). Variations in tree water status were even greater during the nongrowing period, when trees underwent ±18.5 mm of shrinkage and swelling at an average rate of ±75 µm day^{-1} while tree growth is negligible (0.06 mm, 0.2 µm d^{-1}). From the end of the growing season to the end of the year, dehydration (−6.6 mm, −62 µm days^{-1}) exceeded rehydration (6.1 mm, 56 µm days^{-1}), resulting in increased tree water deficit during the winter period. Conversely, rehydration (12.4 mm, 88 µm days^{-1}) was greater

than dehydration (−11.9 mm, 84 µm days^{-1}) before the onset of the growing season, resulting in the net rehydration of stems before growth initiation.

3.3. Average Seasonal Diel Dynamics

The average seasonal diel dynamics of stem radius associated with growth, dehydration, and rehydration are presented in Figure 2 (right column). During the summer, trees grew slower on average (0.3 µm h^{-1}) during the sunshine hours (9:00 to 18:00) compared to the rest of the day (0.7 µm h^{-1}). Tree growth rate increased in the evening, reached its maximum at around 3:00, and gradually declined in the morning until the beginning of the sunny hours (9:00), where it remained more or less constant during the day (9:00 to 18:00). Growth was very slow in the autumn and spring, and null in the winter. In contrast to growth, diurnal patterns in tree water status revealed that trees in summer dehydrated much more markedly during sunny hours and rehydrated mostly in the evening. The diel dynamics of dehydration apparently followed variations in solar radiation intensity during the day. This diurnal dynamic was much less pronounced in spring and autumn and was reversed in winter. Indeed, in winter, trees dehydrated mainly at night, but variations had smaller amplitude than those in the summer. The diurnal dynamics of rehydration during autumn, winter and spring also differed from those during summer. During nongrowing seasons, rehydration exhibited more synchrony with variations in solar radiation intensity during the day. The amplitude of this pattern was larger in the spring (12 µm h^{-1} at 12:00), decreased during the winter (7 µm h^{-1} at 12:00), and was smallest in autumn (3 µm h^{-1} at 12:00).

The diel dynamics of stem shrinkage and swelling in autumn and spring reflect the average observed variation during the gradual autumn dehydration and spring rehydration periods (Figure 2). The observed patterns illustrate how the rehydration of woody tissues is more pronounced in the spring, and that the diel pattern of spring rehydration followed the diel pattern of insolation. In autumn, daily rehydration is comparatively very low, reflecting the gradual net shrinkage of tree stems during this period.

4. Discussion

To our knowledge, this is the first study to document the average hourly, daily, monthly, and seasonal dynamics of tree stem radius associated to growth and tree water status (dehydration and rehydration) on the basis of over a decade of measurements. Our results bring new knowledge, but also confirmed some already formulated hypotheses, described below.

4.1. Average Daily and Monthly Patterns

The growth pattern extracted from the dendrometric signal using the "zero-growth" concept shows dynamics that were consistent with the growth pattern inferred from the cellular analysis of repeatedly sampled wood microcores or pinning techniques [22,23,45], repeatedly sampled dendrometric bands [28], and from continuous growth curves applied to dendrometric data [46,47]. Our results suggest that extracting irreversible growth signals from dendrometric data with this approach adequately represents the dynamics of intra-annual tree ring formation, and has the advantage of documenting both growth dynamics and tree water status at a high temporal resolution.

Our results confirm that tree growth in cold boreal environments occurs over a short period of time, at a faster rate early in the growing season, and gradually decreases until growth stops in late summer [22,35,48]. As previously reported, xylogenesis and intra-annual growth occurred only above a given air temperature threshold [23]. On average, growth onset (DOY 142) and cessation (DOY 260) corresponded to daily average temperatures of 9.9 and 9.7 °C, respectively (Figure 2). These values are very close to the thermal limits for wood formation of 8–9 °C in terms of daily mean air temperature identified from the cellular analysis of weekly sampled wood microcores from conifer species growing in a cold climate [23,45,49]. Similar to previous findings [22], the timing of the maximal growth rate over the year (23–24 June) was synchronous with the maximal day length (20–21 June) and not with the maximal air temperature, which was reached

about 2 weeks later (4–5 July). Maximal day length coincided with the peak in VPD and solar radiation over the year (Figure 2). This reinforces the idea that there is a temperature threshold below which tree growth is inhibited (temperature-limited); however, above this threshold, tree growth depends mainly on solar radiation (sunlight-limited). The latter two parameters were identified as the main fundamental physiological limits to net primary production in boreal forests [50–54]. In addition to the greater source of solar energy associated with longer days and more favourable VPD for tree growth, the hormonal phenology-controlling photoperiod may also play a role in determining the timing of growth onset and the maximal annual growth rate of conifers in cold environments [22,55].

The previously described growth pattern is apparently influenced by temperature and solar radiation constraints on tree growth, which suggests that tree growth is constrained little by soil water availability in these cold, humid forests. Indeed, at the studied latitude, spring snow melt recharged the soil to field capacity early in the growing season, which then decreased throughout the growing season until low evapotranspiration and higher precipitation had contributed to the soil water replenishment in autumn at similar values to those noted in the spring before decreasing again during the winter period, when precipitation was in the form of snow [56,57]. Drought risks are, therefore, particularly low at the beginning of the growing season, when soil water is at field capacity, and air temperatures are cool. If exceptional soil water limitations occur in this cold and humid environment, they are more likely to occur towards the end of the growing season, when soils are dryer, and air temperatures higher. During extreme summer droughts, growth is likely affected by both soil water availability and the effect of other exceptional weather conditions, including air temperature, solar radiation, VPD and relative humidity because these variables affect stomatal and transpiration control [58–60].

Our results also illustrate that, over the course of the year, daily stem radial variations associated with changes in tree water status (dehydration and rehydration) had smaller amplitude during both the growing season and the continuous frost period in winter, and were most pronounced in autumn and particularly in spring (Figure 2). In autumn, tree stems begin to shrink gradually as the temperature cools, solar radiation decreases, and VPD declines, reaching the minimal size during the coldest time of the year (Figure 1). On average over the studied decade, the net shrinkage of stems during this period was 0.5 mm per year, which corresponded with winter stem shrinkage of about 40% of the average annual growth of 1.3 mm per year. Cell dehydration is one of the physiological processes that allow for tree cells to avoid frost damage during the winter dormancy period [61]. However, the mechanism by which trees progressively dehydrate in late autumn, when VPD is near zero and transpiration is inhibited by low air temperature, remains to be documented. During this period, while VPD values are practically zero, large radial variations occur when temperatures warm up and temporarily exceed the freezing point (Figure 1). This suggests that transpiration is also very low [58], if not null during this period, and that the observed variations are rather the result of a freeze/thaw effect or translocation of water in the woody tissues. Similar patterns of large air temperature-dependent variations were observed by others [62–64], who considered this the result of the freeze–thaw cycles of the stem. The mechanisms of bark dehydration to protect living cells from frost damage were proposed to explain these large fluctuations, but the exact mechanism that generates them remains to be elucidated. These occasional large fluctuations could also be the result of an unsuspected methodological artifact. Such artifacts that could significantly affect the results of electronic-dendrometer measurements and signal decomposition seem unlikely (especially during the growing season), but remain to be documented. Whatever the exact cause, a large part of these short-term variations associated with freeze/thaw events should not be interpreted as a real change in the water status of the tree like those associated with variations influenced by VPD, solar radiation, and transpiration during the growing season.

In spring, trees progressively rehydrate with increasing temperatures until they reach the size they had at the end of the previous growing season (Figure 1). The individual

patterns of stem radial variations also reveal large variations associated with freeze/thaw events during this rehydration period as temperatures increase, but VPD values remain low (Figure 1). Following these large fluctuations, the rapid radial expansion of woody tissues before the start of the growing season seems to be predominantly caused by the onset of transpiration and rehydration of woody tissues [58]. Overall, individual stem radial variations in autumn and spring suggest that the short-term fluctuations observed during alternate freeze–thaw periods do not always correspond to a real change in the water status of the trees. Compared to transpiration-driven variations during the growing season, the freeze/thaw or internal translocation of water into woody tissue may be responsible for these large short-term variations. However, it is not always easy to distinguish between true tree dehydration/rehydration and stem shrinkage/swelling effects because they may occur at the same time. In addition, as with progressive stem dehydration in the autumn, the mechanism by which trees gradually rehydrate in early spring while VPD is low, and transpiration is inhibited by low temperatures remains to be documented (Figure 1). Monitoring trees equipped with both sap flow probes and dendrometers would improve our knowledge on the influence of transpiration on tree water status, and would better identify the driving factors of tree radial variation.

4.2. Average Seasonal Diel Dynamics

The effect of temperature and sunlight on tree growth and water status were also illustrated by seasonal diel dynamics (Figure 2). Growth occurs almost exclusively in the summer when air temperature is, on average, above the minimal threshold of 9–10 °C. During summer days, tree growth is minimal during the day, when the stem dehydrates at a rate that follows the normal distribution of daily variation in insolation (centred at noon). Stems then rehydrate in the evening, thus favouring higher growth rates at night. A similar timing of diel stem growth was reported for seven temperate tree species in Europe [31]. These patterns illustrate how trees mainly photosynthesise sugars and assimilate C from solar energy, water, and atmospheric CO_2 during the day, increasing the labile C pool and potentially the C reserve as well; then, they use labile C and oxygen at night to produce energy for the maintenance of physiological process and cell growth, and for cell C allocation through the process of cellular respiration [65,66].

Unlike for growth, which shows variation only in the summer, diel dynamics in tree water status (dehydration and rehydration) differ largely in all seasons (Figure 2). As stems shrink at a rate that follows diel dynamics in insolation during the growing season (mainly in summer), the opposite occurs during the winter, when stems expand during the day and shrink at night. As discussed earlier in relation to annual patterns, this implies that diurnal patterns are not caused by the same mechanism during these two seasons. In winter, diel dynamics also follows variations in solar radiation, but stem radial variation probably does not reflect a real change in tree water status as temperatures are well below the freezing temperature, VPD is nearly zero, and transpiration is most likely inhibited (Figure 2). The diel dynamics observed in winter was likely due to other mechanisms that influenced tree radial variations measured with the electronic dendrometers. Although the inverse diel dynamics of stem radial variations during the cold season (night-time shrinkage and daytime swelling) compared to the growing season was documented [64], the mechanisms behind the diel patterns of stem radial variations in winter remain essentially unknown.

5. Conclusions

High-temporal-resolution dendrometric data and new analytical methods for signal decomposition represent an opportunity to better document variations in tree growth and water status, and identify key environmental drivers. Our analyses of high-temporal-resolution growth data highlight seasonal, monthly, daily, and diel patterns that reflect the influence of the main constraints on forest productivity, namely, temperature and sunlight. This knowledge can be useful in developing hypotheses about the effects of climate change on tree growth in this type of environment. However, our results show that the growth and

water status of balsam fir trees growing in cold and humid environments are controlled by a set of environmental factors through their influence on various physiological processes and mechanisms of which many remain to be elucidated. Work is in progress to model daily tree growth and water status changes from meteorological data to establish quantitative relationships, which is an advancement towards the more accurate modelling of tree growth at high temporal resolutions.

Author Contributions: Conceptualisation: L.D., S.O., D.H. and D.K.; data curation: S.O. and L.D.; formal analysis, software, and visualisation: S.O. and L.D.; investigation: L.D.; methodology and original draft preparation: L.D. and S.O.; project administration and supervision: L.D., D.H., D.K. and N.B.; validation, writing, review, and editing: L.D., S.O., D.H., D.K. and N.B. All authors have read and agreed to the published version of the manuscript.

Funding: This work was funded in part by the Ministère des Ressources naturelles et des Forêts (Québec, Canada), both through project no. 142332064, conducted at the Direction de la recherche forestière and led by L.D., and within the framework of Action 3.6.1.1b of the implementation plan of Québec's Plan pour une économie verte 2030, which aims to acquire knowledge about climate change adaptation. Additional funding was provided by a MITACS Cluster grant (funding reference number IT22943, granted to D.H. and D.K) and by the Contrat de service de recherche forestière obtained by N.B. from the Ministère des Ressources naturelles et des Forêts (Québec, Canada) as part of research project no. 142959361 conducted at the Direction de la recherche forestière (project leader: L.D.), which was coupled with Alliance funding to N.B. (no. ALLRP 570411-21) provided by the Natural Sciences and Engineering Research Council of Canada.

Data Availability Statement: The data presented in this study are available on request from the corresponding author.

Acknowledgments: We thank the field technicians of the *Direction de la recherche forestière* who participated in the deployment and maintenance of the experimental setup.

Conflicts of Interest: The authors declare no conflict of interest.

References

1. Pan, Y.; Birdsey, R.A.; Fang, J.; Houghton, R.; Kauppi, P.E.; Kurz, W.A.; Phillips, O.L.; Shvidenko, A.; Lewis, S.L.; Canadell, J.G.; et al. A Large and Persistent Carbon Sink in the World's Forests. *Science* **2011**, *333*, 988–993. [CrossRef]
2. Friedlingstein, P.; Jones, M.W.; O'Sullivan, M.; Andrew, R.M.; Bakker, D.C.E.; Hauck, J.; Le Quéré, C.; Peters, G.P.; Peters, W.; Pongratz, J.; et al. Global Carbon Budget 2021. *Earth Syst. Sci. Data* **2022**, *14*, 1917–2005. [CrossRef]
3. Cox, P.M.P.M.; Betts, R.A.R.A.; Jones, C.D.C.D.; Spall, S.A.S.A.; Totterdell, I.J.I.J. Acceleration of Global Warming Due to Carbon-Cycle Feedbacks in a Coupled Climate Model. *Nature* **2000**, *408*, 184–187. [CrossRef] [PubMed]
4. Bonan, G.B.G.B. Forests and Climate Change: Forcings, Feedbacks, and the Climate Benefits of Forests. *Science* **2008**, *320*, 1444–1449. [CrossRef] [PubMed]
5. Best, M.J.; Pryor, M.; Clark, D.B.; Rooney, G.G.; Essery, R.; Ménard, C.B.; Edwards, J.M.; Hendry, M.A.; Porson, A.; Gedney, N. The Joint UK Land Environment Simulator (JULES), Model Description–Part 1: Energy and Water Fluxes. *Geosci. Model Dev.* **2011**, *4*, 677–699. [CrossRef]
6. Haverd, V.; Smith, B.; Nieradzik, L.; Briggs, P.R.; Woodgate, W.; Trudinger, C.M.; Canadell, J.G.; Cuntz, M. A New Version of the CABLE Land Surface Model (Subversion Revision R4601) Incorporating Land Use and Land Cover Change, Woody Vegetation Demography, and a Novel Optimisation-Based Approach to Plant Coordination of Photosynthesis. *Geosci. Model Dev.* **2018**, *11*, 2995–3026. [CrossRef]
7. Melton, J.R.; Arora, V.K.; Wisernig-Cojoc, E.; Seiler, C.; Fortier, M.; Chan, E.; Teckentrup, L. CLASSIC v1.0: The Open-Source Community Successor to the Canadian Land Surface Scheme (CLASS) and the Canadian Terrestrial Ecosystem Model (CTEM)–Part 1: Model Framework and Site-Level Performance. *Geosci. Model Dev.* **2020**, *13*, 2825–2850. [CrossRef]
8. Niu, G.; Yang, Z.; Mitchell, K.E.; Chen, F.; Ek, M.B.; Barlage, M.; Kumar, A.; Manning, K.; Niyogi, D.; Rosero, E. The Community Noah Land Surface Model with Multiparameterization Options (Noah-MP): 1. Model Description and Evaluation with Local-scale Measurements. *J. Geophys. Res. Atmos.* **2011**, *116*, 15139. [CrossRef]
9. Sitch, S.; Huntingford, C.; Gedney, N.; Levy, P.E.; Lomas, M.; Piao, S.L.; Betts, R.; Ciais, P.; Cox, P.; Friedlingstein, P. Evaluation of the Terrestrial Carbon Cycle, Future Plant Geography and Climate-carbon Cycle Feedbacks Using Five Dynamic Global Vegetation Models (DGVMs). *Glob. Chang. Biol.* **2008**, *14*, 2015–2039. [CrossRef]
10. Cox, P.M. Emergent Constraints on Climate-Carbon Cycle Feedbacks. *Curr. Clim. Chang. Rep.* **2019**, *5*, 275–281. [CrossRef]

11. Muller, B.; Pantin, F.; Génard, M.; Turc, O.; Freixes, S.; Piques, M.; Gibon, Y. Water Deficits Uncouple Growth from Photosynthesis, Increase C Content, and Modify the Relationships between C and Growth in Sink Organs. *J. Exp. Bot.* **2011**, *62*, 1715–1729. [CrossRef] [PubMed]
12. Fatichi, S.; Leuzinger, S.; Körner, C. Moving beyond Photosynthesis: From Carbon Source to Sink-Driven Vegetation Modeling. *New Phytol.* **2014**, *201*, 1086–1095. [CrossRef] [PubMed]
13. Friend, A.D.; Eckes-Shephard, A.H.; Fonti, P.; Rademacher, T.T.; Rathgeber, C.B.K.; Richardson, A.D.; Turton, R.H. On the Need to Consider Wood Formation Processes in Global Vegetation Models and a Suggested Approach. *Ann. For. Sci.* **2019**, *76*, 49. [CrossRef]
14. Potkay, A.; Trugman, A.T.; Wang, Y.; Venturas, M.D.; Anderegg, W.R.L.; Mattos, C.R.C.; Fan, Y. Coupled Whole-tree Optimality and Xylem Hydraulics Explain Dynamic Biomass Partitioning. *New Phytol.* **2021**, *230*, 2226–2245. [CrossRef]
15. Cabon, A.; Kannenberg, S.A.; Arain, A.; Babst, F.; Baldocchi, D.; Belmecheri, S.; Delpierre, N.; Guerrieri, R.; Maxwell, J.T.; McKenzie, S. Cross-Biome Synthesis of Source versus Sink Limits to Tree Growth. *Science* **2022**, *376*, 758–761. [CrossRef] [PubMed]
16. Cabon, A.; Anderegg, W.R.L. Turgor-Driven Tree Growth: Scaling-up Sink Limitations from the Cell to the Forest. *Tree Physiol.* **2022**, *42*, 225–228. [CrossRef] [PubMed]
17. Gea-Izquierdo, G.; Guibal, F.; Joffre, R.; Ourcival, J.M.; Simioni, G.; Guiot, J. Modelling the Climatic Drivers Determining Photosynthesis and Carbon Allocation in Evergreen Mediterranean Forests Using Multiproxy Long Time Series. *Biogeosciences* **2015**, *12*, 3695–3712. [CrossRef]
18. Hayat, A.; Hacket-Pain, A.J.; Pretzsch, H.; Rademacher, T.T.; Friend, A.D. Modeling Tree Growth Taking into Account Carbon Source and Sink Limitations. *Front. Plant Sci.* **2017**, *8*, 182. [CrossRef]
19. Hartmann, F.P.; Rathgeber, C.B.K.; Fournier, M.; Moulia, B. Modelling Wood Formation and Structure: Power and Limits of a Morphogenetic Gradient in Controlling Xylem Cell Proliferation and Growth. *Ann. For. Sci.* **2017**, *74*, 14. [CrossRef]
20. Brienen, R.J.W.; Caldwell, L.; Duchesne, L.; Voelker, S.; Barichivich, J.; Baliva, M.; Ceccantini, G.; Di Filippo, A.; Helama, S.; Locosselli, G.M. Forest Carbon Sink Neutralized by Pervasive Growth-Lifespan Trade-Offs. *Nat. Commun.* **2020**, *11*, 4241. [CrossRef]
21. Babst, F.; Friend, A.D.; Karamihalaki, M.; Wei, J.; Von Arx, G.; Papale, D.; Peters, R.L. Modeling Ambitions Outpace Observations of Forest Carbon Allocation. *Trends Plant Sci.* **2021**, *26*, 210–219. [CrossRef] [PubMed]
22. Rossi, S.; Deslauriers, A.; Anfodillo, T.; Morin, H.; Saracino, A.; Motta, R.; Borghetti, M. Conifers in Cold Environments Synchronize Maximum Growth Rate of Tree-ring Formation with Day Length. *New Phytol.* **2006**, *170*, 301–310. [CrossRef] [PubMed]
23. Rossi, S.; Deslauriers, A.; Griçar, J.; Seo, J.W.; Rathgeber, C.B.K.; Anfodillo, T.; Morin, H.; Levanic, T.; Oven, P.; Jalkanen, R. Critical Temperatures for Xylogenesis in Conifers of Cold Climates. *Glob. Ecol. Biogeogr.* **2008**, *17*, 696–707. [CrossRef]
24. Cuny, H.E.; Rathgeber, C.B.K.; Frank, D.; Fonti, P.; Mäkinen, H.; Prislan, P.; Rossi, S.; Del Castillo, E.M.; Campelo, F.; Vavrčík, H. Woody Biomass Production Lags Stem-Girth Increase by over One Month in Coniferous Forests. *Nat. Plants* **2015**, *1*, 15160. [CrossRef]
25. Dao, M.C.E.; Rossi, S.; Walsh, D.; Morin, H.; Houle, D. A 6-Year-Long Manipulation with Soil Warming and Canopy Nitrogen Additions Does Not Affect Xylem Phenology and Cell Production of Mature Black Spruce. *Front. Plant Sci.* **2015**, *6*, 877. [CrossRef]
26. Lenz, A.; Hoch, G.; Körner, C. Early Season Temperature Controls Cambial Activity and Total Tree Ring Width at the Alpine Treeline. *Plant Ecol. Divers.* **2013**, *6*, 365–375. [CrossRef]
27. Huang, J.-G.J.-G.; Zhang, Y.; Wang, M.; Yu, X.; Deslauriers, A.; Fonti, P.; Liang, E.; Mäkinen, H.; Oberhuber, W.; Rathgeber, C.B.K.C.B.K.; et al. A Critical Thermal Transition Driving Spring Phenology of Northern Hemisphere Conifers. *Glob. Chang. Biol.* **2023**, *29*, 1606–1617. [CrossRef]
28. Dow, C.; Kim, A.Y.; D'Orangeville, L.; Gonzalez-Akre, E.B.; Helcoski, R.; Herrmann, V.; Harley, G.L.; Maxwell, J.T.; McGregor, I.R.; McShea, W.J. Warm Springs Alter Timing but Not Total Growth of Temperate Deciduous Trees. *Nature* **2022**, *608*, 552–557. [CrossRef] [PubMed]
29. D'Orangeville, L.; Itter, M.; Kneeshaw, D.; Munger, J.W.; Richardson, A.D.; Dyer, J.M.; Orwig, D.A.; Pan, Y.; Pederson, N. Peak Radial Growth of Diffuse-Porous Species Occurs during Periods of Lower Water Availability than for Ring-Porous and Coniferous Trees. *Tree Physiol.* **2022**, *42*, 304–316. [CrossRef]
30. Zweifel, R.; Haeni, M.; Buchmann, N.; Eugster, W. Are Trees Able to Grow in Periods of Stem Shrinkage? *New Phytol.* **2016**, *211*, 839–849. [CrossRef]
31. Zweifel, R.; Sterck, F.; Braun, S.; Buchmann, N.; Eugster, W.; Gessler, A.; Häni, M.; Peters, R.L.; Walthert, L.; Wilhelm, M. Why Trees Grow at Night. *New Phytol.* **2021**, *231*, 2174–2185. [CrossRef] [PubMed]
32. Salomón, R.L.; Peters, R.L.; Zweifel, R.; Sass-Klaassen, U.G.W.; Stegehuis, A.I.; Smiljanic, M.; Poyatos, R.; Babst, F.; Cienciala, E.; Fonti, P. The 2018 European Heatwave Led to Stem Dehydration but Not to Consistent Growth Reductions in Forests. *Nat. Commun.* **2022**, *13*, 28. [CrossRef] [PubMed]
33. Peters, R.L.; Steppe, K.; Cuny, H.E.; De Pauw, D.J.W.; Frank, D.C.; Schaub, M.; Rathgeber, C.B.K.; Cabon, A.; Fonti, P. Turgor–a Limiting Factor for Radial Growth in Mature Conifers along an Elevational Gradient. *New Phytol.* **2021**, *229*, 213–229. [CrossRef]
34. Cabon, A.; Peters, R.L.; Fonti, P.; Martínez-Vilalta, J.; De Cáceres, M. Temperature and Water Potential Co-limit Stem Cambial Activity along a Steep Elevational Gradient. *New Phytol.* **2020**, *226*, 1325–1340. [CrossRef] [PubMed]

35. Oogathoo, S.; Duchesne, L.; Houle, D.; Kneeshaw, D. Characterizing Seasonal Radial Growth Dynamics of Balsam Fir in a Cold Environment Using Continuous Dendrometric Data: A Case Study in a 12-Year Soil Warming Experiment. *Sensors* **2022**, *22*, 5155. [CrossRef]
36. MFFP Classification Écologique Du Territoire Québécois. Available online: https://www.donneesquebec.ca/recherche/dataset/systeme-hierarchique-de-classification-ecologique-du-territoire (accessed on 1 March 2023).
37. Kottek, M.; Grieser, J.; Beck, C.; Rudolf, B.; Rubel, F. World Map of the Köppen-Geiger Climate Classification Updated. *Meteorol. Zeitschrift* **2006**, *15*, 259–263. [CrossRef]
38. Delisle, J.; Bernier-Cardou, M.; Labrecque, A. Extreme Cold Weather Causes the Collapse of a Population of Lambdina Fiscellaria (Lepidoptera: Geometridae) in the Laurentian Mountains of Québec, Canada. *Can. Entomol.* **2019**, *151*, 311–328. [CrossRef]
39. Houle, D.; Lajoie, G.; Duchesne, L. Major Losses of Nutrients Following a Severe Drought in a Boreal Forest. *Nat. Plants* **2016**, *2*, 16187. [CrossRef]
40. D'Orangeville, L.; Houle, D.; Côté, B.; Duchesne, L. Soil Response to a 3-Year Increase in Temperature and Nitrogen Deposition Measured in a Mature Boreal Forest Using Ion-Exchange Membranes. *Environ. Monit. Assess.* **2014**, *186*, 8191–8202. [CrossRef]
41. D'Orangeville, L.; Côté, B.; Houle, D.; Morin, H.; Duchesne, L. Increased Soil Temperature and Atmospheric N Deposition Have No Effect on the N Status and Growth of a Mature Balsam Fir Forest. *Biogeosciences* **2013**, *10*, 4627–4639. [CrossRef]
42. D'Orangeville, L.; Côté, B.; Houle, D.; Whalen, J. Reduced Mineralizable Carbon in a Boreal Forest Soil after Three Years of Artificial Warming. *Can. J. Soil Sci.* **2013**, *93*, 567–572. [CrossRef]
43. D'Orangeville, L.; Côté, B.; Houle, D.; Morin, H.; Duchesne, L. A Three-Year Increase in Soil Temperature and Atmospheric N Deposition Has Minor Effects on the Xylogenesis of Mature Balsam Fir. *Trees* **2013**, *27*, 1525–1536. [CrossRef]
44. Tumajer, J.; Scharnweber, T.; Smiljanic, M.; Wilmking, M. Limitation by Vapour Pressure Deficit Shapes Different Intra-annual Growth Patterns of Diffuse-and Ring-porous Temperate Broadleaves. *New Phytol.* **2022**, *233*, 2429–2441. [CrossRef] [PubMed]
45. Deslauriers, A.; Rossi, S.; Anfodillo, T.; Saracino, A. Cambial Phenology, Wood Formation and Temperature Thresholds in Two Contrasting Years at High Altitude in Southern Italy. *Tree Physiol.* **2008**, *28*, 863–871. [CrossRef] [PubMed]
46. Duchesne, L.; Houle, D.; D'Orangeville, L. Influence of Climate on Seasonal Patterns of Stem Increment of Balsam Fir in a Boreal Forest of Québec, Canada. *Agric. For. Meteorol.* **2012**, *162*, 108–114. [CrossRef]
47. Miller, T.W.; Stangler, D.F.; Larysch, E.; Honer, H.; Seifert, T.; Kahle, H.-P. A Methodological Framework to Optimize Models Predicting Critical Dates of Xylem Phenology Based on Dendrometer Data. *Dendrochronologia* **2022**, *72*, 125940. [CrossRef]
48. Rossi, S.; Anfodillo, T.; Čufar, K.; Cuny, H.E.E.; Deslauriers, A.; Fonti, P.; Frank, D.; Gričar, J.; Gruber, A.; Huang, J.-G.; et al. Pattern of Xylem Phenology in Conifers of Cold Ecosystems at the Northern Hemisphere. *Glob. Chang. Biol.* **2016**, *22*, 3804–3813. [CrossRef] [PubMed]
49. Rossi, S.; Deslauriers, A.; Anfodillo, T.; Carraro, V. Evidence of Threshold Temperatures for Xylogenesis in Conifers at High Altitudes. *Oecologia* **2007**, *152*, 1–12. [CrossRef] [PubMed]
50. Boisvenue, C.; Running, S.W. Impacts of Climate Change on Natural Forest Productivity–Evidence since the Middle of the 20th Century. *Glob. Chang. Biol.* **2006**, *12*, 862–882. [CrossRef]
51. Allen, C.D.; Macalady, A.K.; Chenchouni, H.; Bachelet, D.; McDowell, N.; Vennetier, M.; Kitzberger, T.; Rigling, A.; Breshears, D.D.; Hogg, E.H.T. A Global Overview of Drought and Heat-Induced Tree Mortality Reveals Emerging Climate Change Risks for Forests. *For. Ecol. Manag.* **2010**, *259*, 660–684. [CrossRef]
52. Nemani, R.R.; Keeling, C.D.; Hashimoto, H.; Jolly, W.M.; Piper, S.C.; Tucker, C.J.; Myneni, R.B.; Running, S.W. Climate-Driven Increases in Global Terrestrial Net Primary Production from 1982 to 1999. *Science* **2003**, *300*, 1560–1563. [CrossRef]
53. Running, S.W.; Nemani, R.R.; Heinsch, F.A.; Zhao, M.; Reeves, M.; Hashimoto, H. A Continuous Satellite-Derived Measure of Global Terrestrial Primary Production. *Bioscience* **2004**, *54*, 547–560. [CrossRef]
54. Churkina, G.; Running, S.W. Contrasting Climatic Controls on the Estimated Productivity of Global Terrestrial Biomes. *Ecosystems* **1998**, *1*, 206–215. [CrossRef]
55. Huang, J.G.; Ma, Q.; Rossi, S.; Biondi, F.; Deslauriers, A.; Fonti, P.; Liang, E.; Mäkinen, H.; Oberhuber, W.; Rathgeber, C.B.K.; et al. Photoperiod and Temperature as Dominant Environmental Drivers Triggering Secondary Growth Resumption in Northern Hemisphere Conifers. *Proc. Natl. Acad. Sci. USA* **2020**, *117*, 20645–20652. [CrossRef]
56. Houle, D.; Bouffard, A.; Duchesne, L.; Logan, T.; Harvey, R. Projections of Future Soil Temperature and Water Content for Three Southern Quebec Forested Sites. *J. Clim.* **2012**, *25*, 7690–7701. [CrossRef]
57. D'Orangeville, L.; Houle, D.; Duchesne, L.; Côté, B. Can the Canadian Drought Code Predict Low Soil Moisture Anomalies in the Mineral Soil? An Analysis of 15 Years of Soil Moisture Data from Three Forest Ecosystems in Eastern Canada. *Ecohydrology* **2016**, *9*, 238–247. [CrossRef]
58. Oogathoo, S.; Houle, D.; Duchesne, L.; Kneeshaw, D. Vapour Pressure Deficit and Solar Radiation Are the Major Drivers of Transpiration of Balsam Fir and Black Spruce Tree Species in Humid Boreal Regions, Even during a Short-Term Drought. *Agric. For. Meteorol.* **2020**, *291*, 108063. [CrossRef]
59. Oogathoo, S.; Houle, D.; Duchesne, L.; Kneeshaw, D. Tree Transpiration Well Simulated by the Canadian Land Surface Scheme (CLASS) but Not during Drought. *J. Hydrol.* **2022**, *604*, 127196. [CrossRef]
60. Duchesne, L.; Houle, D. Modelling Day-to-Day Stem Diameter Variation and Annual Growth of Balsam Fir (Abies Balsamea (L.) Mill.) from Daily Climate. *For. Ecol. Manage.* **2011**, *262*, 863–872. [CrossRef]

61. Havranek, W.M.; Tranquillini, W. Physiological Processes during Winter Dormancy and Their Ecological Significance. In *Ecophysiology of Coniferous Forests*; Smith, W.K., Hinckley, T.M., Eds.; Academic Press: Cambridge, MA, USA, 1995; pp. 95–124.
62. Zweifel, R.; Häsler, R. Frost-Induced Reversible Shrinkage of Bark of Mature Subalpine Conifers. *Agric. For. Meteorol.* **2000**, *102*, 213–222. [CrossRef]
63. Améglio, T.; Cochard, H.; Ewers, F.W. Stem Diameter Variations and Cold Hardiness in Walnut Trees. *J. Exp. Bot.* **2001**, *52*, 2135–2142. [CrossRef] [PubMed]
64. Dong, M.; Jiang, Y.; Zhang, W.; Yang, Y.; Yang, H. Effect of Alpine Treeline Conditions on the Response of the Stem Radial Variation of Picea Meyeri Rebd. et Wils to Environmental Factors. *Polish J. Ecol.* **2011**, *59*, 729–739.
65. Raven, J.A. The Quantitative Role of 'Dark'Respiratory Processes in Heterotrophic and Photolithotrophic Plant Growth. *Ann. Bot.* **1976**, *40*, 587–602. [CrossRef]
66. Amthor, J.S. The Role of Maintenance Respiration in Plant Growth. *Plant. Cell Environ.* **1984**, *7*, 561–569.